Exosomes from normal cartilage endplate stem cells ameliorate intervertebral disc degeneration more effectively than exosomes from degenerated cartilage endplate stem cell by activating the AKT/autophagy pathway

Liwen Luo (1661854388@qq.com)
Xinqiao Hospital
Xiuying Jian
Chongqing Medical University
Hui Sun
Army Military Medical University
Jinghao Qin
Army Military Medical University
Yanqiu Wang
Army Military Medical University
Di Yang
Army Military Medical University
Changqing Li
Army Military Medical University
MingHan Liu
Army Military Medical University
Zhiqiang Tian
Army Military Medical University
Yue Zhou
Army Military Medical University

Research

Keywords: Intervertebral disc degeneration, Cartilage endplate stem cells, Exosome; Autophagy, Apoptosis

Posted Date: June 12th, 2020

DOI: https://doi.org/10.21203/rs.3.rs-33698/v1

Abstract

Background

Nucleus pulposus cells (NPCs) apoptosis is an important factor in exacerbating intervertebral disc degeneration (IVDD) that can be effectively suppressed by exosomes. The aim of this study was to reaearch whether normal cartilage endplate stem cells (CESCs) derived exosomes (N-Exos) were more conducive to activation of autophagy and inhibition of NPCs apoptosis and IVDD than degenerated CESCs derived exosomes (D-Exos) or not.

Methods

Rat CESCs were isolated and identified, and the exosomes produced by normal CESCs and degenerated CESCs were extracted. The bioinformatics differences between normal CESCs derived exosomes (N-Exos) and degenerated CESCs derived exosome (D-Exos) were analyzed by mass spectrometry, heat map and KEGG enrichment analysis biology. The effects of N-Exos and D-Exos on the inhibition of NPCs apoptosis were examined by TUNEL staining, flow cytometry and western blotting. The involvement of the AKT and autophagy signaling pathways was investigated using the signaling inhibitor LY294002. Magnetic resonance imaging, western blotting and immunofluorescence staining were used to evaluate the therapeutic effects of N-Exos in vivo.

Results

CESCs in the cartilage endplate (CEP) could secrete a large amount of exosomes. N-Exos were more conducive to activation of autophagy than D-Exos. The apoptotic rate of NPCs was decreased obviously after treatment with N-Exos than after D-Exos treatment. N-Exos inhibited NPCs apoptosis or attenuated IVDD in a rat tail model by activating the AKT and autophagy signaling pathways.

Conclusions

It was the first to confirm that CEP could delay the progression of IVDD through exosomes secreted by normal CESCs. The therapeutic effects of N-Exos on inhibiting NPCs apoptosis and slowing IVDD progression was more effective than D-Exos by activating the PI3K/AKT/autophagy pathway, which explained the reason that the incidence of IVDD was increased after inflammation of the CEP.

Background

Intervertebral disc degeneration (IVDD) is a common cause of lower back pain, limits activity[1] and is usually characterized by upregulation of matrix metalloproteinase (MMP) and proinflammatory cytokine expression, a reduction in the number of functional nucleus pulposus cells (NPCs) and anatomical and

morphological changes[2, 3]. The important mechanism by which IVDD occurs is through not only a reduction in the nutrient supply from cartilage endplates (CEP) to the inner layer of the annulus fibrosus and NPCs[4] but also weakened CEP-mediated regulation of IVDD-associated anabolism and catabolism[5], leading to NPCs senescence and apoptosis.

The CEP is a hyaline cartilage located on the upper and lower sides of the intervertebral disc. Previous studies showed that there were a large number of progenitor cells that differentiated into osteoblasts, adipocytes and chondrocytes in human CEP tissues, and these progenitor cells were defined as cartilage endplate stem cells (CESCs)[6]. It has been demonstrated that CESCs perform powerful functions in inhibiting IVDD by promoting NPCs regeneration and regulating the homeostasis of the intervertebral disc[7–9]. However, the detailed mechanism remains unclear. In animal experiments, mesenchymal stem cells (MSCs) or adipose stem cells showed great potential in treating IVDD by secreting exosomes. For example, exosomes from MSCs could modulate endoplasmic reticulum stress and ameliorate IVDD in vivo[10]. Considering that CESCs shared some MSC-like characteristics, we hypothesized that CESCs might also secrete exosomes to regulate the homeostasis of the microenvironment and inhibit the progression of IVDD. And studies had shown that after inflammation and degeneration of CEP, IVDD was more likely to occur, but the mechanisms are unclear. Therefore, we also performed mass spectrometry analysis and bioinformatics analysis on normal CESCs derived exosomes (N-Exos) and degenerated CESCs derived exosomes (D-Exos) to elucidate the reason why the incidence of IVDD was increased after inflammation of the CEP and the mechanism of cartilage endplate inhibiting IVDD.

Exosomes are extracellular vesicles with diameters of 30–150 nm. After being released from cells, such as liver cells, MSCs, and tumor cells, exosomes transport membrane components, proteins, microRNAs and mRNAs into the intracellular environment upon fusion with the cytoplasmic membrane[11, 12] and then exert therapeutic effects on liver ischemia-reperfusion injury and degenerative diseases through cell-to-cell communication, cell signaling and metabolism modulation[13–15]. Researches showed that inflammation and degeneration of CEP could accelerate IVDD, but IVDD are thought to be repaired via conversion normal CESCs into NPCs or by strengthening the nutrient supply of intervertebral discs via normal CEP[5, 16]. Moreover, until now it is unclear whether normal CESCs can secrete exosomes and what role secreted exosomes play in IVDD. Studies have shown that transplantation of exosomes secreted by MSCs into intervertebral discs could ameliorate IVDD by promoting proliferation and differentiation and inhibiting apoptosis of NPCs[17, 18]. Therefore, we mainly investigated whether exosomes secreted by CESCs (CESC-Exos) had a therapeutic effect on IVDD and the specific regulatory mechanism of the therapeutic effect. Recent research showed that macrophage-derived exosomes could activate autophagy during osteogenic differentiation and bone regeneration[19]. Additionally, human umbilical cord MSC-derived exosomes could exert antiapoptotic effects by activating the autophagy-related signaling pathway phosphatidylinositol 3-kinase (PI3K)/AKT/mTOR[20]. Therefore, we hypothesized that N-Exos might be more effective in inhibiting NPCs apoptosis and ameliorating IVDD by activating intracellular autophagy pathways than D-Exos.

Autophagy, an essential intracellular catabolic process, contributes to intracellular quality control and maintains cell survival by degrading and recycling damaged components and toxic proteins and organelles under inflammatory, nutrient deprivation and stress conditions[21–23]. Autophagy can inhibit the expression of senescence-associated secretory phenotype (SASP) proteins or degrade apoptotic proteins to regulate the progression of various diseases, such as cancer[24], neurodegenerative diseases and osteoarthritis[25, 26]. For example, studies associated with neuronal aging showed that neuronal cells exhibited significant SASPs after inhibition of autophagy to degrade GATA4. In IVDD, enhancing autophagy by activating the PI3K/p-AKT signaling pathway can significantly reduce the expression level of SASP proteins, such as IL-6, IL-1β and TNFα, and inhibit aging and apoptosis[27, 28]. Moreover, it has been showed that exosomes derived from MSCs promote autophagy and inhibit apoptosis[19, 20]. Therefore, we hypothesized that N-Exos might also inhibit NPCs apoptosis by activating the PI3K/AKT/autophagy signaling pathway.

In this study, we analyzed the differences in bioinformatics between N-Exos and D-Exos and investigated the inhibitory effect of N-Exos on IVDD. We showed for the first time that normal CESCs could secrete a large number of exosomes and inhibit NPCs apoptosis in vitro and in vivo. Mechanistic experiments showed that N-Exos could activate effectively the PI3K/p-AKT/autophagy signaling pathway and inhibit NPCs apoptosis and IVDD compared to D-Exos. Our study offers new insights into IVDD treatment strategies using N-Exos as a therapeutic tool.

Materials And Methods

Reagents and antibodies

The AKT inhibitor (LY294002) was obtained from Beyotime (Shanghai, China). Antibodies against Caspase3, Bax, Bcl-2, Beclin-1, GAPDH, p-ERK1/2, p-AKT, Tsg101 and Alix were purchased from Proteintech (Wuhan, China). Antibodies against AKT, ERK1/2, JNK/p-JNK and NFκB/p-NFκB were obtained from Abcam (Cambridge, MA, USA). Antibodies against LC3A/B were purchased from KleanAB (Shanghai, China). Antibodies against LC3B were purchased from Bioss (Beijing, China). Collagenase II was purchased from Sangon Biotech (Shanghai, China). Tert-butyl hydroperoxide (TBHP) and PKH67 were obtained from Sigma (St. Louis, MO, USA). 1,1’-Dioctadecyl-3,3,3’,3‘-tetramethylindotricarbocyanine iodide (DIR) was obtained from Invitrogen (Carlsbad, CA, USA). MSC osteogenic differentiation medium, chondrogenic differentiation medium and adipogenic differentiation medium were provided by Cyagen (Guangzhou, China).

Rat IVDD model and reagent treatment

Male SD rats (n = 40) were obtained from the Experimental Animal Center of the Army Military Medical University (ChongQing, China). A total of 32 adult male rats (12 weeks old) were used for the in vivo experiment and were equally divided into 4 groups of 8 rats: control group, LY294002 (20 μmol) group, exosome (40 μg) group, and LY294002 (20 μmol) + exosome (40 μg) group. At the third week after the operation, the NP tissue was extracted from the treatment site of 5 rats in each group for western blotting.

At the sixth week after the operation, we performed magnetic resonance imaging (MRI) and immunofluorescence staining of the treatment sites of the remaining 3 rats in each group. A total of 8 young male rats (aged 3-4 weeks) were used for isolation and extraction of CESCs and NPCs. After the rats were anesthetized with 5% chloral hydrate, the caudal discs (C5/6, C6/7 and C7/8) were randomly transversely injected with 20 μmol of LY294002 or 40 μg of exosomes in each site in the experimental group every week for 6 weeks. Animal use and experimental procedures met the requirements of the Guidelines for the Care and Use of Laboratory Animals of the National Institutes of Health and were approved by the Animal Care and Use Committee of the Army Medical University.

CESCs and NPCs isolation and characterization

Ten young rats were obtained and killed by cervical dislocation after anesthetization. Six to eight segments of caudal vertebrae NP tissue were obtained from the caudal root with a surgical tip blade. The skin was removed from the rat tails, and the tails were then sterilized by iodine immersion. The fiber ring of the intervertebral disc was cut with a surgical blade to obtain a normal rat intervertebral disc. The NP tissues and CEP tissues were cut into 1 mm^3 pieces and placed in a cell culture flask. Next, 4 ml of 0.2% collagenase type 2 was added, and the tissues were gently shaken and digested at 37°C for 1-2 hours and filtered through a 70 μm filter. After the cells were centrifuged and the supernatant was removed, rat NPCs were collected, seeded in cell culture flasks and cultured in DMEM F12 medium containing 20% fetal bovine serum at 5% CO_2 and 37°C.

Osteogenic, adipogenic and chondrogenic differentiation

CESCs were cultured in 6-well plates for osteogenic differentiation. The osteogenic differentiation medium (MUBMX-90021, Cyagen Biosciences, Guangzhou, China) was changed every 3 days for a total of 2-3 weeks. The cells were washed twice with PBS, fixed with 2 ml of 4% neutral formaldehyde solution for 20 minutes at room temperature and stained with 1% Alizarin Red S solution for 30 minutes, and osteogenesis was evaluated under a microscope (Olympus, Japan). CESCs were cultured in 6-well plates for adipogenic differentiation. The adipogenic differentiation medium was replaced every 3 days, the cells were then cultured with medium B (MUBMX-90031, Cyagen) for 1 day, and this cycle was repeated for a total of 3 weeks. The cells were washed twice with PBS, fixed with 2 ml of 4% neutral formaldehyde solution for 20 minutes and stained with Oil Red O working solution for 30 minutes, and adipogenesis was evaluated under a microscope. For chondrogenic differentiation, CESCs were centrifuged, incubated in a centrifuge tube at 37°C in 5% CO_2 for 24-48 hours and then incubated in chondrogenic differentiation medium (MUCMX-9004, Cyagen) for 21 days. To estimate chondrogenesis, the chondrified micromass was fixed with 4% formaldehyde, embedded in paraffin, sliced at a thickness of 4 μm, and then stained with Alcian blue for observation under a microscope.

Exosome isolation and characterization

Third- to fifth-generation CESCs in good condition were selected to extract exosomes. After the cells reached 80% confluence, the culture supernatant was collected 3 days later to extract normal CESCs

derived exosomes or the culture supernatant of CESCs treated with 80umol/ml TBHP was collected 3 days later to extract degenerated CESCs derived exosomes. The supernatant was centrifuged at 2 000 × g for 10 minutes at 4°C to remove cell debris and was then centrifuged at 110 000 × g for 70 minutes at 4°C to isolate the exosomes. The supernatant was carefully removed, and the exosome pellet was resuspended by repeatedly pipetting with 1 ml of PBS. Then, a 0.22 μm filter membrane was used for filter sterilization. The sample was centrifuged again at 110 000 × g for 70 minutes and washed once, and the exosome pellet was collected in 200 μl of PBS. Five microliters of PKH67 or DIR was added to 500 μl of diluent to form the reaction liquid, and 100 μl of exosomes was added to the reaction liquid. After 10 minutes, 5% BSA was added to stop the reaction, and then exosomes labeled with different membrane dyes were obtained. The size and concentration of exosomes were measured by nanoparticle tracking analysis (NTA) (Wayen Biotechnologies, Shanghai). Exosome morphology was examined by electron microscopy, and the purity and characteristics were analyzed by western blot (WB) analysis based on the expression of exosome markers (Tsg101 and Alix).

Transmission electron microscopy (TEM)

The cells were separated by trypsin digestion and fixed with 2% glutaraldehyde at 4°C for 2 days. Then, the samples were treated with 1% osmate for 30 minutes. Next, 50%, 70%, 80% and 100% ethanol gradient dehydration was performed. After the samples were soaked in a 100% acetone/Epon 812 (Shell Chemical Co, Houston, TX) solution, ultrathin sections (60 nm) were prepared, stained with 5% uranium acetate for 30-60 minutes, washed twice with double-distilled water, and stained with lead citrate for 10 minutes. The samples were washed three times with double-distilled water and observed under a Tecnai-10 transmission electron microscope (Philips, Amsterdam, Netherlands).

Western blotting

After the cells were lysed in RIPA buffer containing the protease inhibitor PMSF, the protein concentration was determined, and 4 × Laemmli sample buffer (Catalog: 161074, BIO-RAD) was added to the sample. Electrophoresis was performed at 150 V with 4-20% gradient gels. Semidry transfer electrophoresis was performed for 7 minutes at 2.5 V. After the membrane was sealed, the antibody was added to detect the target protein, and the membrane was incubated at 4°C with shaking overnight. The membrane was washed with PBS, diluted second antibody was added and incubated for 1.5 hours, and the membrane was washed again. The ECL working solution (Millipore, MO, USA) was prepared by mixing solutions A and B at a ratio of 1:1. The membrane surface was covered with working solution, placed in the imaging system (Bio-Rad, USA), and pictures were taken.

TUNEL staining

The apoptosis-related TUNEL staining kit (Beyotime, Shanghai, China) was used to detect the level of apoptosis according to the protocol. The level of apoptosis was indicated by red staining in the nucleus. Different areas of the sample were randomly selected and captured under a fluorescence microscope (Olympus, Tokyo, Japan) to count the number of TUNEL-positive cells.

Immunofluorescence staining

When the NPCs reached 60% confluence, the cells were washed with PBS 2-3 times. Then, a 0.3% hydrogen peroxide/formaldehyde solution was added, and the cells were incubated for 10 minutes at room temperature, permeabilized with 0.2% Triton for 5 minutes, and blocked with 5% BSA for 60 minutes. After the specific primary antibody was added, the samples were incubated at 4°C overnight. The specimens were washed with PBS 3 times and incubated with the fluorescently labeled secondary antibody at 37°C for 60 minutes. After the nuclei were stained with DAPI, images of the specimens were captured using a fluorescence microscope (Olympus, Japan) or laser confocal microscope (Lexia, Japan).

Flow cytometry to detect apoptosis and identify CESCs

The Annexin V-APC/PI apoptosis detection kit (BD Biosciences, CA, USA) was used to detect and assess the rate of apoptosis via flow cytometry. The cells were digested and collected with 0.25% Trypsin-EDTA, washed with PBS, resuspended in 100 μl of binding buffer and stained with 5 μl of Annexin V-APC and 5 μl of 7-AAD. After the cells were incubated for 30 minutes at room temperature, the apoptosis rate of the cells was detected in a flow cytometer (BD Biosciences, CA, USA). FlowJo software was used to analyze the collected data. To identify CESCs, antibodies against CD44 (103,005, Biolegend, San Diego, CA, USA), CD90 (202,503, Biolegend), and CD45 (103,107, Biolegend) were used. CESCs were collected within three generations and washed 3 times with PBS. After the cells were incubated at room temperature for 30 minutes and washed with PBS, the percentage of CESCs was detected and analyzed by flow cytometry (BD FACSCalibur, USA).

Magnetic resonance imaging

At six weeks after the operation, the signal and structural changes in the disc were assessed by a 7.0 T animal magnet (Bruker Pharmascan, Germany) based on the sagittal T2-weighted images. To obtain clear imaging results, the parameters of the T2-weighted sections were set as previously described[29]**.** The severity of IVDD was analyzed in a double-blind manner according to the Pfirrmann grading system[30].

Data analysis

All data are presented as the mean±S.D. of at least three independent experiments. One-way analysis of variance (ANOVA) followed by Tukey's test for comparisons between the two groups was used to analyze and compare the results with GraphPad Prism 7.0 (GraphPad Software Inc., CA, USA). P values <0.05 were considered statistically significant.

Results

CESCs in CEP secrete exosomes

Based on previous studies demonstrating the presence of a large number of CESCs in the CEP of humans and mice, we investigated whether there were CESCs in rat CEP. We extracted CESCs from 3- to 4-week-old rats and identified CESCs by osteogenic, chondrogenic, and adipogenic differentiation (Fig. 1a-b). The flow cytometry results showed that most CESCs positively expressed the stem cell surface markers CD90 and CD44 and did not express the differentiated cell surface marker CD45 (Fig. 1c). After enrichment and extraction, the exosomes secreted by CESCs were identified by analyzing the morphology, size and marker proteins of the exosomes by TEM, NTA and WB analysis, respectively (Fig. 1d-f). The results demonstrated that rat CESCs have functions similar to those of other types of stem cells that could secrete a large number of exosomes.

Normal CESCs derived exosomes (N-Exos) were more conducive to activation of autophagy than degenerated CESCs derived exosomes (D-Exos)

Since the incidence of IVDD increased after inflammation or degeneration of CEP, we analyzed the differences in the regulation of cell signaling pathways and functions of exosomes secreted by normal CESCs or TBHP-induced degenerated CESCs. Mass spectrometry and heat map analysis of the obtained N-Exos and D-Exos, we found that there was a clear difference between the proteins carried by the N-Exos and D-Exos (Fig. 2a). KEGG enrichment analysis and Gene Ontology (GO) data analysis of proteins contained in N-Exos and D-Exos respectively, the results showed that N-Exos and D-Exos had differences in regulating cell biological functions, such as regulating cell phagosome and leukocyte transendothelial migration (Fig. 2b-e). Further KEGG enrichment analysis of top 50 quantitative differential proteins between N-Exos and D-Exos (Fig. 2f), we known that N-Exos were more conducive to activation of autophagy than D-Exos, which indicated that N-Exos might suppress IVDD by regulating and activating autophagy.

Normal CESCs derived exosomes (N-Exos) was more effective in attenuating rat NPCs apoptosis than degenerated CESCs derived exosomes (N-Exos)

Normal CEP and CESCs can inhibit NPCs apoptosis by providing nutrients, inhibiting the inflammatory response and differentiating into NPCs. However, whether it is possible to inhibit NPCs apoptosis by secreting exosomes is not clear. We isolated, extracted and cultured rat NPCs (Fig. 3a). Then, rat NPCs were identified by high expression of collagen II and low expression of collagen I (Fig. 3b). N-Exos and NPCs were cocultured, and we found that exosomes can be taken up into the cytoplasm by NPCs (Fig. 3c). Mass spectrometry analysis and Gene Ontology (GO) data analysis of the differential proteins between N-Exos and D-Exos revealed that there were many important proteins in the N-Exos that negatively regulated apoptosis (Fig. 3d). Therefore, NPCs were treated with NC (0ug/ml), D-Exos (40ug/ml) and N-Exos (40ug/ml) to verify that antiapoptotic effects of N-Exos was more effective. TUNEL staining and flow cytometry analysis of apoptosis suggested that in the presence of 40 μg/ml N-Exos, fewer NPCs underwent apoptosis (Fig. 3e-f). Representative western blotting and quantitative analysis of Caspase3, Bax and Bcl-2 expression in NPCs also showed that N-Exos had antiapoptotic

effects, and the antiapoptotic effect was more obvious with increasing concentrations of exosomes (Fig. 3g).

Normal CESCs derived exosomes (N-Exos) was more effective of regulating autophagic flux and inhibit apoptosis in rat NPCs than degenerated CESCs derived exosomes (D-Exos)

There were reports that exosomes could attenuate diabetic nephropathy and D-GaIN/LPS-induced hepatocyte injury by promoting autophagic flux and inhibiting apoptosis[31, 32]. Therefore, we also examined whether exosomes could inhibit NPCs apoptosis by promoting autophagic flux. Mass spectrometry and KEGG enrichment analysis of the all differential proteins carried in the extracted N-Exos and D-Exos revealed that N-Exos might also inhibit NPCs apoptosis by activating autophagy (Fig. 4a). To verify this finding, we divided the NPCs into four groups for different treatments: NC, TBHP, TBHP + D-Exos and TBHP + N-Exos. LC3-B and Caspase3 immunofluorescence double staining results showed that apoptotic protein expression was increased in cells treated with TBHP, but this increase in autophagosome fluorescence intensity and apoptotic protein expression were reversed in cells treated with TBHP + D-Exos or TBHP + N-Exos (Fig. 4b). Although the number of autophagosomes increased in NPCs treated with TBHP + D-Exos or TBHP + N-Exos compared with the NC group or NPCs treated with TBHP, the number of autophagosomes was the largest in TBHP + N-Exos group as observed by TEM (Fig. 4c). Additionally, we found that the LC3B/A ratio and level of the autophagy-associated protein Beclin-1 were increased and the apoptosis-related proteins Caspase3 and Bax were reduced in NPCs treated with TBHP + D-Exos or TBHP + N-Exos, especially TBHP + N-Exos group, compared with the NPCs treated with TBHP (Fig. 4d). These results suggested that N-Exos could inhibit NPCs apoptosis by regulating autophagic flow, and it was better than D-Exos.

Normal CESCs derived exosomes (N-Exos) inhibit NPCs apoptosis by activating the PI3K/AKT/autophagy signaling pathway

MSC-Exos were previously shown to be effective in repairing critical size osteochondral defects via activation of AKT and ERK signaling in an immunocompetent rat model[33]. Based on the results of KEGG enrichment analysis (Fig. 4a), we hypothesized that N-Exos might also activate autophagy through the PI3K/AKT pathway. We treated NPCs with NC, D-Exos and N-Exos and found that the p-AKT signaling pathway was activated when NPCs were treated N-Exos. We then examined other signaling pathways, such as p-ERK1/2 and p-JNK, but there were no significant changes (Fig. 5a). Moreover, we found that the apoptotic rate of NPCs and the apoptotic protein expression of Caspase3 and Bax decreased significantly, and the ratio of the autophagy protein LC3B/A, the level of p-AKT increased after activation of the p-AKT signaling pathway, but the above effect was inhibited by the AKT inhibitor LY294002 (20 μmol/ml treatment for three days) (Fig. 5b-c). Immunofluorescence staining of p-AKT and TUNEL staining also led to the conclusion that N-Exos could inhibit NPCs by activating the PI3K/AKT/autophagy signaling pathway (Fig. 5d).

Normal CESCs derived exosomes (N-Exos) alleviate the progression of IVDD in rats

To confirm that exosomes can be injected into the intervertebral disc, we labeled exosomes with DIR and then performed live imaging. We found that DIR-labeled N-Exos (DIR-N-Exos) had a signal in the IVD than unlabeled exosomes after three days (Fig. 6a). To further confirm the conclusion that N-Exos could inhibit NPCs apoptosis and ameliorate IVDD by activating the AKT/autophagy pathway, we divided the rats into four groups: the NC group, LY294002 group (20 μmol), N-Exos group, and N-Exos + LY204002 group. MRI of the treatment site was performed after four weeks. The results suggested that the PI3K/AKT inhibitor LY294002 exacerbated the progression of IVDD, and exosomes alleviated disc degeneration, but LY294002 attenuated exosome-mediated inhibition of the progression of IVDD (Fig. 6b). We extracted NP tissue from the treatment site at the third week after the operation for western blotting. The results showed that compared with those of the control group, the ratio of LC3B/A and the level of p-AKT in the LY294002 group were significantly reduced, and the ratio of LC3B/A and the level of p-AKT in the exosome group were significantly increased, but the inhibitor LY294002 could inhibit exosome-mediated promotion of NPCs autophagy and activation of the AKT pathway (Fig. 6c). The immunofluorescence staining results also showed that exosomes inhibited the expression of Caspase3 and activated the AKT/autophagy pathway, but LY294002 attenuated these effects of N-Exos (Fig. 6d-e). In short, we demonstrated that N-Exos can inhibit NPCs apoptosis by activating autophagy via the PI3K/AKT signaling pathway in vivo.

Discussion

Exosomes are extracellular vesicles that can effectively deliver substances and are widely used in the treatment of various diseases. Through participating in intercellular communication and the modulation of cellular processes, exosomes can effectively inhibit the progression of IVDD[17, 33]. Recent studies on exosomes have focused on exosomes derived from MSCs, adipose stem cells and tumor cells. No one had studied exosomes secreted by stem cells present in the CEP. In this work, we first proposed that cartilage endplate stem cells (CESCs) in the rat cartilage endplates (CEP) located on the upper and lower sides of the intervertebral disc (IVD) could secrete exosomes. Moreover, normal CESCs derived exosomes were more conducive to activation of autophagy than degenerated CESCs derived exosomes. Compared to mesenchymal stem cells (MSCs), although CESCs located near IVD are difficult to obtain, CESCs can better simulate the repair process of pathological changes in IVDD via activating AKT/autophagy pathway and inhibiting NPCs apoptosis.

Previous studies have shown that as the main source of nutrient transport from vertebral marrow to the IVD[34], the CEP plays an important role in suppressing IVDD, but whether this function is performed through exosomes derived from CESCs has not been studied. We extracted and cultured CESCs to obtain the cell supernatant. According to a previous method for extracting exosomes, CESCs secrete a large amount of exosomes. Therefore, we hypothesized that CESCs might have similar functions as those of MSCs and could regulate disease progression by secreting exosomes. Considering the fact that after inflammation and degeneration of CEP, IVDD was more likely to occur. Therefore, we analyzed the difference between N-Exos and D-Exos in regulating cell signaling pathways and functions. The results found N-Exos were more conducive to activation of autophagy than D-Exos, which showed that N-Exos

might inhibit IVDD via activating autophagy. This might explain the reason why the incidence of IVDD was increased after inflammation of the CEP, which was that the degenerated CESCs derived exosomes had a reduced ability to activate autophagy. Through GO analysis of proteins carried in exosomes, we found that N-Exos might inhibit IVDD by inhibiting NPCs apoptosis. We then performed TUNEL staining, flow cytometry and western blotting experiments to detect the effect of N-Exos on apoptosis inhibition. The results confirmed that N-Exos could inhibit NPCs apoptosis effectively than D-Exos. This provided a new direction for us to examine treatments for IVDD; for example, it was possible to construct engineered exosomes that overexpressed a protein that inhibits IVDD to strengthen the therapeutic effect.

Previous studies have suggested that exosomes are endogenously produced and secreted by host cells and might serve as a system for delivering proteins or RNA; further, exosomes are involved in intercellular crosstalk and interorganelle communication[35]. For example, studies have shown that MSC-derived exosomes inhibit ischemic myocardial cell apoptosis and promote cardiac endothelial microvascular regeneration or bone regeneration by enhancing autophagy[19, 36]; however, we did not know whether N-Exos also inhibited NPCs apoptosis by activating autophagy. KEGG enrichment analysis of N-Exos and D-Exos revealed that the effect of N-Exos on activating autophagy to inhibit NPCs apoptosis was more effective compared with D-Exos. Immunofluorescence staining, TEM analysis and western blotting results also confirmed that exosomes, especially N-Exos, could inhibit TBHP-induced apoptosis by activating autophagy. Considering that the PI3K/AKT signaling pathway was significantly enhanced in the KEGG enrichment analysis, the signaling pathway through which exosome activate autophagy was verified. As the NPCs treated with NC, D-Exos and N-Exos, the expression of p-AKT was significantly increased compared with the expression of ERK1/2, p-ERK1/2, JNK and p-JNK in the N-Exos group. Moreover, western blotting, flow cytometry and TUNEL staining results showed that compared with the effect in the control group, the AKT signaling pathway was effectively inhibited in the presence of the AKT pathway inhibitor LY294002, but the AKT signaling pathway was effectively activated in the presence of N-Exos. Furthermore, LY294002 could inhibit exosome-mediated activation of the AKT signaling pathway. After activation of the PI3K/AKT signaling pathway, the levels of the apoptotic proteins Caspase3 and Bax in NPCs were significantly reduced, but the expression levels of the antiapoptotic protein Bcl-2 increased. These findings show that N-Exos mainly activate autophagy in NPCs by enhancing the p-AKT signaling pathway, thereby inhibiting NPCs apoptosis.

To clarify the function of exosomes in vivo, we used a rat model and injected exosomes and the PI3K/AKT inhibitor LY294002 into the rat tail disc. By injecting DIR-labeled N-Exos into the IVD and performing live imaging three days later, we found that N-Exos could stay in the IVD for a longer period of time. By analyzing the MRI, western blotting and immunofluorescence results, we found that after injection of LY294002, the expression of Caspase3 increased and IVDD was accelerated. However, after the injection of N-Exos, expression of the apoptotic protein Caspase3 was significantly reduced, and IVDD was inhibited, but exosome-mediated inhibition of IVDD could be effectively reversed by LY294002. These results indicate that exosomes derived from CESCs can enter NPCs to inhibit disc degeneration by enhancing autophagy through activation of the PI3K/AKT signaling pathway in vivo.

Conclusions

In summary, the present work demonstrated that there were a large number of CESCs in the rat CEP that can secrete exosomes. Furthermore, N-Exos can inhibit NPCs apoptosis and weaken disc degeneration more effectively than D-Exos by promoting autophagy through activation of the PI3K/AKT signaling pathway both in vitro and in vivo. These results provide further support for the importance of exosomes derived from normal CESCs as therapeutic tools for IVDD prevention and treatment.

Abbreviations

MSCs: Mesenchymal stem cells; CEP: Cartilage endplate; CESCs: Cartilage endplate stem cells; COL1: Collagen type I; COL2: Collagen type II; IVD: Intervertebral disc; IVDD: Intervertebral disc degeneration.

Declarations

Acknowledgements

We thank all **authors** involved in the study and are grateful to the Animal Center of Army Military Medical University (Third Military Medical University) for providing the rats.

Author Contributions

Yue Zhou, Zhiqiang Tian and Minghan Liu are Co-corresponding.

Liwen Luo: Conception and design, Conducting experiments, Collection and/or assembly of data, Data analysis and interpretation manuscript writing.

Jinghao Qin and Xiuying Jian: Conducting experiments, Collection and/or assembly of data.

Hui Sun and Yanqiu Wang: Provision of study material, Data analysis.

Di Yang and Changqing Li: Conducting experiments, Animal modeling assistance.

Minghan Liu: Revised the manuscript, Administrative support, Financial support.

Zhiqiang Tian: Revised the manuscript, Final approval of manuscript, Administrative support, Data analysis and interpretation, Financial support.

Yue Zhou: Revised the manuscript, Final approval of manuscript, Conception and design, Manuscript revision, Financial support. All authors read and approved the final manuscript.

Funding: This work was supported by the National Natural Science Foundation of China (Grant Number: 81874028); the Research Program of Foundation Science and Application Technology of Chongqing

(Grant Number: cstc2018jcyjA1826) and Basic Medical College Foundation of Army Medical University (2019JCZX10).

Availability of data and materials

All data generated or analyzed during this study are included in this published article.

Ethics approval and consent to participate

Animal use and experimental procedures met the requirements of the Guidelines for the Care and Use of Laboratory Animals of the National Institutes of Health and were approved by the Animal Care and Use Committee of the Army Medical University

Consent for publication

Not applicable

Conflicts of interest

The authors declare no conflicts of interest.

References

1. Andersson GB. Epidemiological features of chronic low-back pain. Lancet. 1999;354(9178):581–5.
2. Urban JP, Roberts S. Degeneration of the intervertebral disc. Arthritis research therapy. 2003;5(3):120–30.
3. Wang F, Gao ZX, Cai F, Sinkemani A, Xie ZY, Shi R, Wei JN, Wu XT. Formation, function, and exhaustion of notochordal cytoplasmic vacuoles within intervertebral disc: current understanding and speculation. Oncotarget. 2017;8(34):57800–12.
4. Wong J, Sampson SL, Bell-Briones H, Ouyang A, Lazar AA, Lotz JC, Fields AJ. Nutrient supply and nucleus pulposus cell function: effects of the transport properties of the cartilage endplate and potential implications for intradiscal biologic therapy. Osteoarthritis cartilage. 2019;27(6):956–64.

5. Li FC, Zhang N, Chen WS, Chen QX. Endplate degeneration may be the origination of the vacuum phenomenon in intervertebral discs. Medical hypotheses. 2010;75(2):169–71.
6. Liu LT, Huang B, Li CQ, Zhuang Y, Wang J, Zhou Y. Characteristics of stem cells derived from the degenerated human intervertebral disc cartilage endplate. PloS one. 2011;6(10):e26285.
7. Wang H, Zhou Y, Huang B, Liu LT, Liu MH, Wang J, Li CQ, Zhang ZF, Chu TW, Xiong CJ. Utilization of stem cells in alginate for nucleus pulposus tissue engineering. Tissue engineering Part A. 2014;20(5–6):908–20.
8. Chen S, Zhao L, Deng X, Shi D, Wu F, Liang H, Huang D, Shao Z. Mesenchymal Stem Cells Protect Nucleus Pulposus Cells from Compression-Induced Apoptosis by Inhibiting the Mitochondrial Pathway. Stem cells international. 2017;2017:9843120.
9. Wang W, Wang Y, Deng G, Ma J, Huang X, Yu J, Xi Y, Ye X: **Transplantation of Hypoxic-Preconditioned Bone Mesenchymal Stem Cells Retards Intervertebral Disc Degeneration via Enhancing Implanted Cell Survival and Migration in Rats**. *Stem cells international* 2018, **2018**:7564159.
10. Liao Z, Luo R, Li G, Song Y, Zhan S, Zhao K, Hua W, Zhang Y, Wu X, Yang C. Exosomes from mesenchymal stem cells modulate endoplasmic reticulum stress to protect against nucleus pulposus cell death and ameliorate intervertebral disc degeneration in vivo. Theranostics. 2019;9(14):4084–100.
11. Montecalvo A, Larregina AT, Shufesky WJ, Stolz DB, Sullivan ML, Karlsson JM, Baty CJ, Gibson GA, Erdos G, Wang Z, et al. Mechanism of transfer of functional microRNAs between mouse dendritic cells via exosomes. Blood. 2012;119(3):756–66.
12. Nojima H, Freeman CM, Schuster RM, Japtok L, Kleuser B, Edwards MJ, Gulbins E, Lentsch AB: **Hepatocyte exosomes mediate liver repair and regeneration via sphingosine-1-phosphate**. *Journal of hepatology* 2016, **64**(1):60–68.
13. Phinney DG, Pittenger MF. Concise Review: MSC-Derived Exosomes for Cell-Free Therapy. Stem cells. 2017;35(4):851–8.
14. Nong K, Wang W, Niu X, Hu B, Ma C, Bai Y, Wu B, Wang Y, Ai K. Hepatoprotective effect of exosomes from human-induced pluripotent stem cell-derived mesenchymal stromal cells against hepatic ischemia-reperfusion injury in rats. Cytotherapy. 2016;18(12):1548–59.
15. Xia C, Zeng Z, Fang B, Tao M, Gu C, Zheng L, Wang Y, Shi Y, Fang C, Mei S, et al. Mesenchymal stem cell-derived exosomes ameliorate intervertebral disc degeneration via anti-oxidant and anti-inflammatory effects. Free Radic Biol Med. 2019;143:1–15.
16. He Z, Jia M, Yu Y, Yuan C, Wang J. Roles of SDF-1/CXCR4 axis in cartilage endplate stem cells mediated promotion of nucleus pulposus cells proliferation. Biochem Biophys Res Commun. 2018;506(1):94–101.
17. Cheng X, Zhang G, Zhang L, Hu Y, Zhang K, Sun X, Zhao C, Li H, Li YM, Zhao J. Mesenchymal stem cells deliver exogenous miR-21 via exosomes to inhibit nucleus pulposus cell apoptosis and reduce intervertebral disc degeneration. J Cell Mol Med. 2018;22(1):261–76.

18. Lu K, Li HY, Yang K, Wu JL, Cai XW, Zhou Y, Li CQ. Exosomes as potential alternatives to stem cell therapy for intervertebral disc degeneration: in-vitro study on exosomes in interaction of nucleus pulposus cells and bone marrow mesenchymal stem cells. Stem Cell Res Ther. 2017;8(1):108.
19. Wei F, Li M, Crawford R, Zhou Y, Xiao Y. Exosome-integrated titanium oxide nanotubes for targeted bone regeneration. Acta biomaterialia. 2019;86:480–92.
20. Liu H, Sun X, Gong X, Wang G. Human umbilical cord mesenchymal stem cells derived exosomes exert antiapoptosis effect via activating PI3K/Akt/mTOR pathway on H9C2 cells. Journal of cellular biochemistry. 2019;120(9):14455–64.
21. Klionsky DJ, Abdelmohsen K, Abe A, Abedin MJ, Abeliovich H, Acevedo Arozena A, Adachi H, Adams CM, Adams PD, Adeli K, et al: **Guidelines for the use and interpretation of assays for monitoring autophagy** (**3rd edition**). *Autophagy* 2016, **12**(1):1-222.
22. Mizushima N, Komatsu M. Autophagy: renovation of cells and tissues. Cell. 2011;147(4):728–41.
23. Levine B, Kroemer G. Autophagy in the pathogenesis of disease. Cell. 2008;132(1):27–42.
24. Weiner LM, Lotze MT. Tumor-cell death, autophagy, and immunity. N Engl J Med. 2012;366(12):1156–8.
25. Guo F, Liu X, Cai H, Le W. Autophagy in neurodegenerative diseases: pathogenesis and therapy. Brain pathology. 2018;28(1):3–13.
26. Luo P, Gao F, Niu D, Sun X, Song Q, Guo C, Liang Y, Sun W. The Role of Autophagy in Chondrocyte Metabolism and Osteoarthritis: A Comprehensive Research Review. BioMed research international. 2019;2019:5171602.
27. Yang S, Zhang F, Ma J, Ding W. Intervertebral disc ageing and degeneration: The antiapoptotic effect of oestrogen. Ageing Res Rev. 2020;57:100978.
28. Guo F, Zou Y, Zheng Y. Moracin M inhibits lipopolysaccharide-induced inflammatory responses in nucleus pulposus cells via regulating PI3K/Akt/mTOR phosphorylation. Int Immunopharmacol. 2018;58:80–6.
29. Chen J, Xie JJ, Jin MY, Gu YT, Wu CC, Guo WJ, Yan YZ, Zhang ZJ, Wang JL, Zhang XL, et al. Sirt6 overexpression suppresses senescence and apoptosis of nucleus pulposus cells by inducing autophagy in a model of intervertebral disc degeneration. Cell death disease. 2018;9(2):56.
30. Che YJ, Guo JB, Liang T, Chen X, Zhang W, Yang HL, Luo ZP. Assessment of changes in the micro-nano environment of intervertebral disc degeneration based on Pfirrmann grade. The spine journal: official journal of the North American Spine Society. 2019;19(7):1242–53.
31. Zhao S, Liu Y, Pu Z. Bone marrow mesenchymal stem cell-derived exosomes attenuate D-GalN/LPS-induced hepatocyte apoptosis by activating autophagy in vitro. Drug Des Devel Ther. 2019;13:2887–97.
32. Jin J, Shi Y, Gong J, Zhao L, Li Y, He Q, Huang H. Exosome secreted from adipose-derived stem cells attenuates diabetic nephropathy by promoting autophagy flux and inhibiting apoptosis in podocyte. Stem Cell Res Ther. 2019;10(1):95.

33. Zhang S, Chuah SJ, Lai RC, Hui JHP, Lim SK, Toh WS. MSC exosomes mediate cartilage repair by enhancing proliferation, attenuating apoptosis and modulating immune reactivity. Biomaterials. 2018;156:16–27.
34. Huang YC, Urban JP, Luk KD. Intervertebral disc regeneration: do nutrients lead the way? Nature reviews Rheumatology. 2014;10(9):561–6.
35. Zappulli V, Friis KP, Fitzpatrick Z, Maguire CA, Breakefield XO. Extracellular vesicles and intercellular communication within the nervous system. J Clin Investig. 2016;126(4):1198–207.
36. Gong XH, Liu H, Wang SJ, Liang SW, Wang GG. Exosomes derived from SDF1-overexpressing mesenchymal stem cells inhibit ischemic myocardial cell apoptosis and promote cardiac endothelial microvascular regeneration in mice with myocardial infarction. Journal of cellular physiology. 2019;234(8):13878–93.

Figures

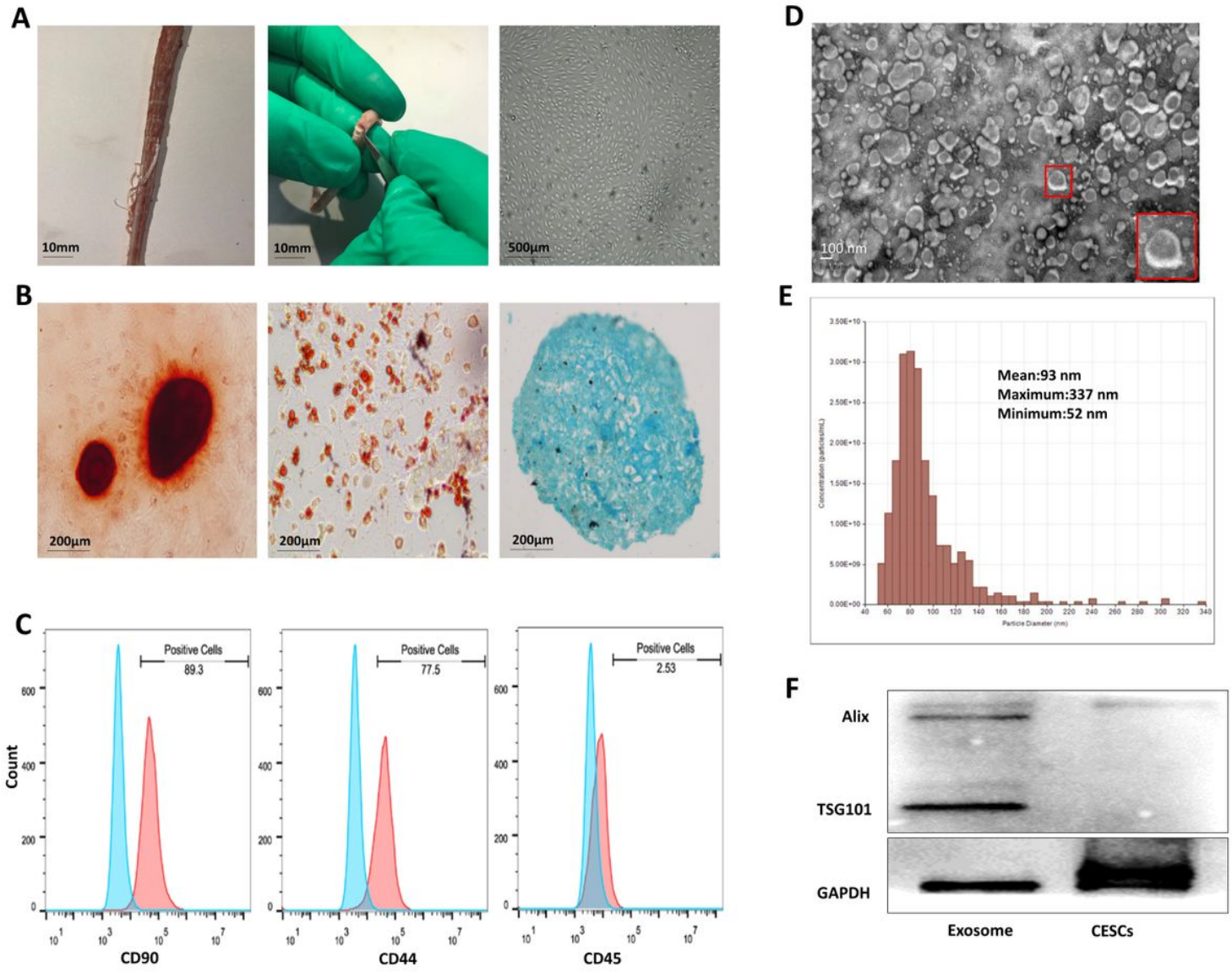

Figure 1

Identification of rat cartilage end plate stem cells (CESCs) and CESCs derived exosomes (CESCs-Exos). a Horizontal views of rat CEP and the morphology of P3 CESCs at 100% confluence. b After osteogenic induction for 14 days (left panel), adipogenic induction for 15 days (middle panel) and chondrogenic induction for 21 days (right panel), the ability of CESCs to differentiate into different cell lines was confirmed by Alizarin Red staining, Oil Red O staining and Alcian blue staining, respectively. c Cell surface markers (CD90, CD44 and CD45) of CESCs were detected by flow cytometric analysis. The red curves represent the fluorescence intensity of CESCs stained with the corresponding antibodies. d TEM images were used to identify the morphology of CESCs-Exos. e Nanoparticle trafficking analysis (NTA) was used to analyze the particle size distribution of CESCs-Exos. f Representative western blots showing Alix and TSG101 expression in CESCs-Exos and CESCs.

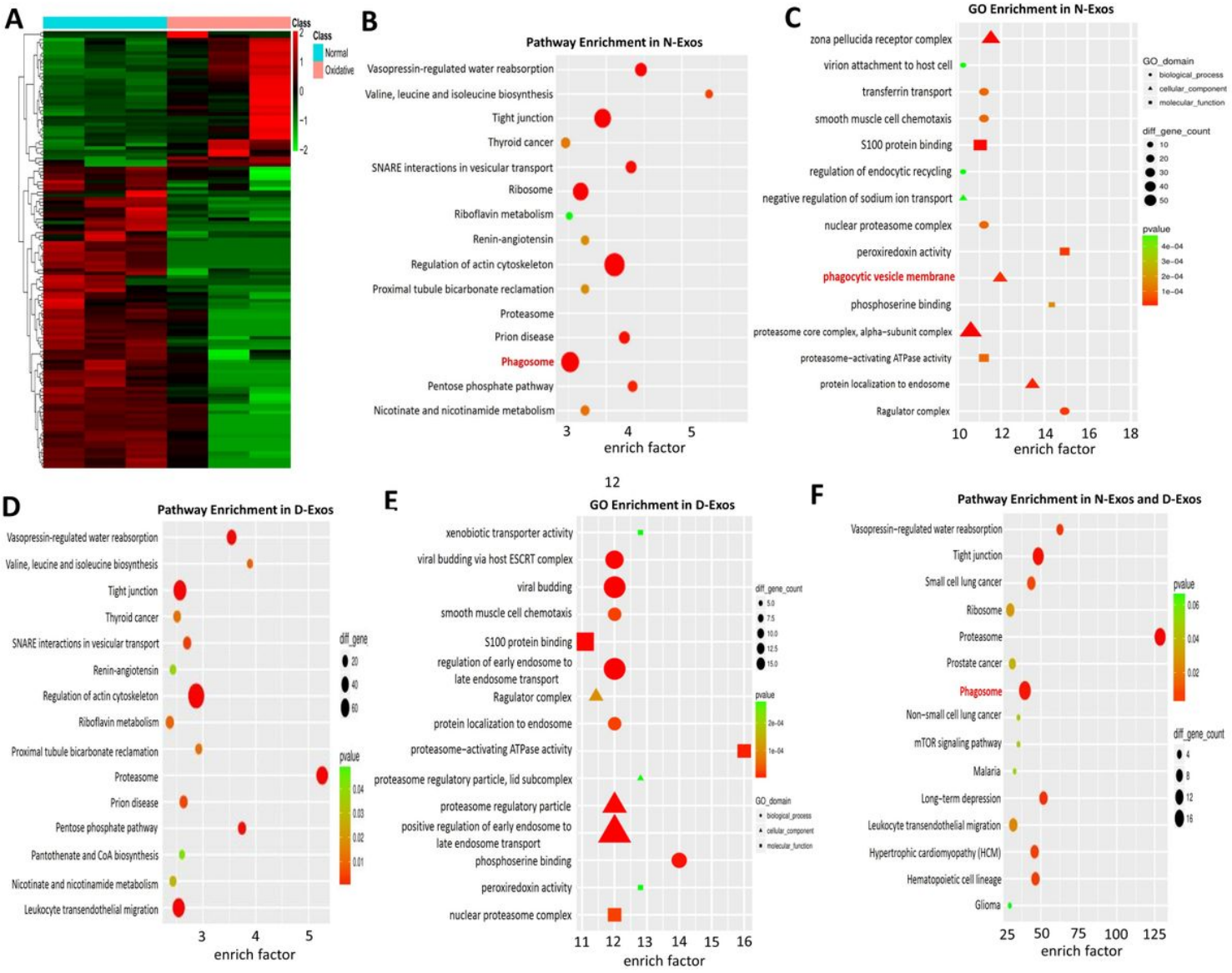

Figure 2

Bioinformatics Analysis between normal CESCs derived exosomes (N-Exos) and degenerated CESCs derived exosomes (D-Exos). a Heat map analysis of differential proteins between N-Exos and D-Exos. b KEGG enrichment analysis of proteins contained in N-Exos. c KEGG enrichment analysis of proteins contained in D-Exos. d KEGG enrichment analysis of top 50 quantitative differential proteins between N-Exos and D-Exos.

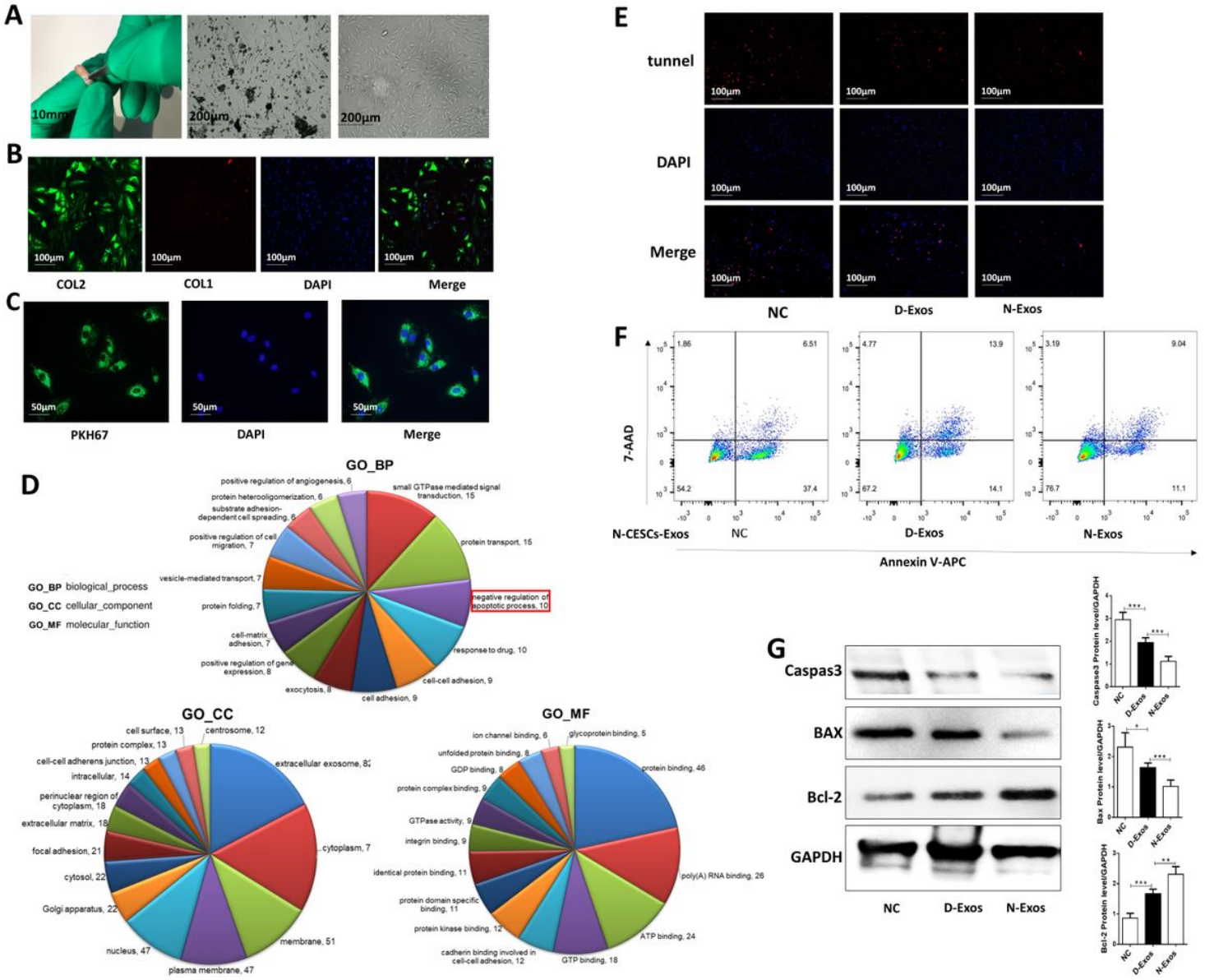

Figure 3

N-Exos was more effective in inhibiting apoptosis compared with D-Exos. a Morphological observations of rat NP tissue (left panel), P1 NPCs at 50% confluence (middle panel) and P3 NPCs at 100% confluence (middle panel). b Double immunofluorescence staining of collagen II (green) and collagen I (red) in NPCs. c Representative images of NPCs incubated with PBS or PKH67-labeled N-Exos for 24 hours. d Gene Ontology (GO) analysis of the all differential proteins carried in the normal CESCs derived exosomes (N-Exos) and degenerated CESCs derived exosomes (D-Exos). e-g TUNEL staining, flow cytometry, representative western blots and quantitative data of Caspase3, Bax and Bcl-2 expression in NPCs treated

with NC (0ug/ml), D-Exos (40ug/ml) and N-Exos (40ug/ml). NC: Normal Control; ns: P>0.05; * p < .05; ** p < .01; *** p < .001.

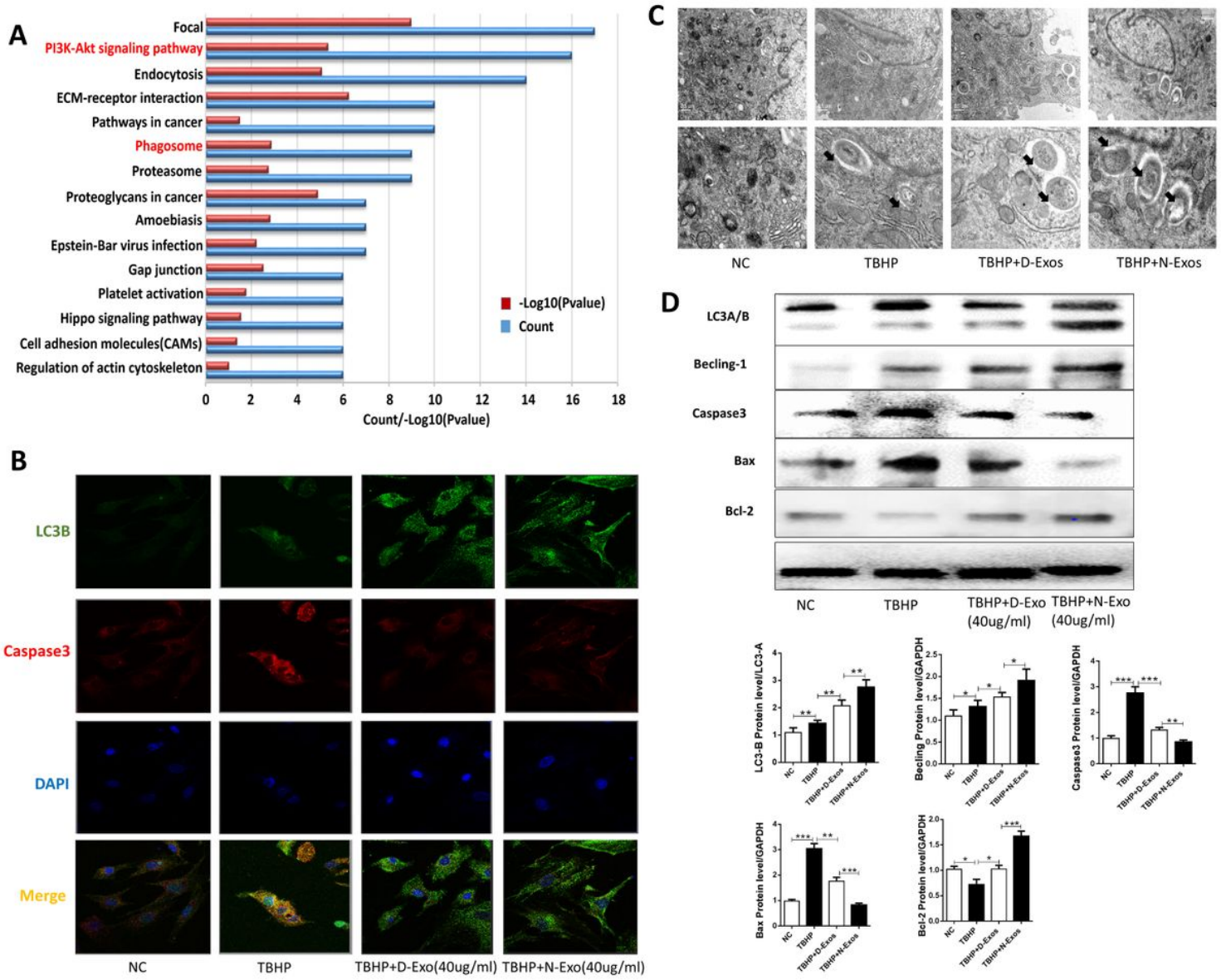

Figure 4

N-Exos was more effective of promoting NPCs autophagy and inhibiting apoptosis than D-Exos. a KEGG enrichment analysis of the all differential proteins carried in the normal CESCs derived exosomes (N-Exos) and degenerated CESCs derived exosomes (D-Exos). b Double immunofluorescence staining of LC3-B (green) and Caspase3 (red) in NPCs treated with NC (0ug/ml), TBHP (80umol/ml), TBHP (80umol/ml)+D-Exos (40μg/ml) or TBHP(80umol/ml)+N-Exos (40μg/ml). c Autophagosomes (black arrow: autophagosome) were examined by TEM after NPCs were treated as described above. d Representative western blots and quantitative data of LC3A/B, Beclin-1, Caspase3, Bax and Bcl-2 expression in NPCs treated with NC, TBHP (80umol/ml), TBHP (80umol/ml)+D-Exos (40μg/ml) or TBHP (80umol/ml)+N-Exos (40μg/ml). NC: Normal Control; ns: P>0.05; * p < .05; ** p < .01; *** p < .001.

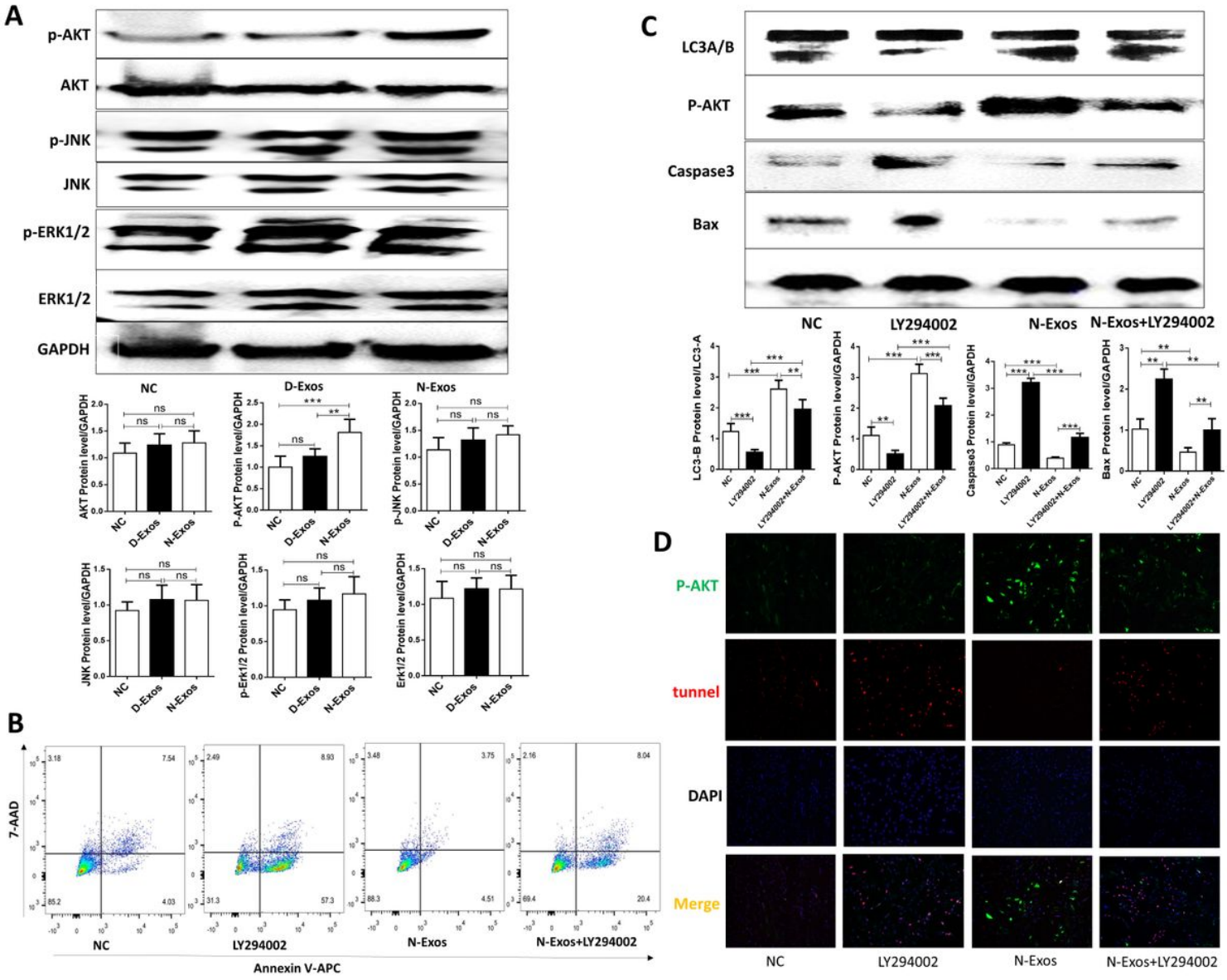

Figure 5

Normal CESCs derived exosomes (N-Exos) inhibited NPCs apoptosis by activating the PI3K/AKT/autophagy signaling pathway. a Western blot analysis and quantitative data of p-AKT, AKT, p-JNK, JNK p-ERK1/2 and ERK1/2 expression in NPCs treated with NC (0ug/ml), D-Exos (40ug/ml) and N-Exos (40ug/ml). b Flow cytometry was used to detect apoptosis of NPCs treated with NC (0μg/ml)., LY294002 (20μmol/ml), N-Exo (40μg/ml) and LY294002 (20μmol/ml)+N-Exos (40 μg/ml). c-d Representative western blots and quantitative data of LC3A/B, p-AKT, Caspase3 and Bax expression and double immunofluorescence staining of p-AKT (green) and TUNEL (red) in NPCs treated as described above. NC: Normal Control; ns: P>0.05; * p < .05; ** p < .01; *** p < .001.

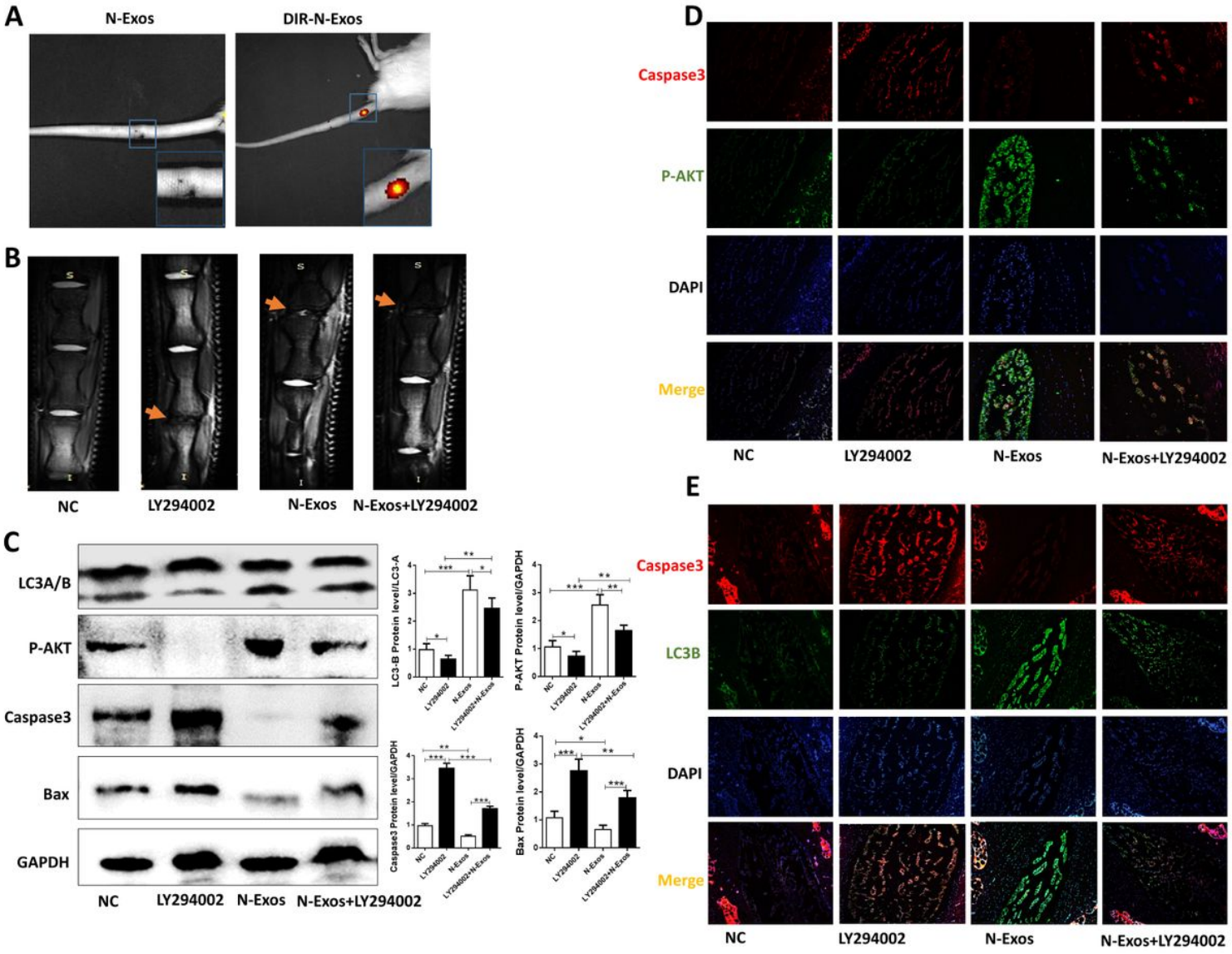

Figure 6

Normal CESCs derived exosomes (N-Exos) alleviated the progression of IVDD in vivo. a In vivo imaging of rat IVDs and vertebral segments treated with unlabeled N-Exos (N-Exos) or DIR-labeled N-Exos (DIR-N-Exos). b Representative MRI images of rat intervertebral discs treated with NC (0μg/ml)., LY294002 (20μmol/ml), N-Exos (40 μg/ml) and N-Exos (40 μg/ml)+LY294002 (20μmol/ml). c Western blots and quantitative data of LC3A/B, p-AKT, Caspase3 and Bax expression in the rat intervertebral disc at the third week after treatment. d-e Representative images of double immunofluorescence staining of Caspase3 (red) and p-AKT (green) (d) and Caspase3 (red) and LC3B (green) (e) in rat discs in each group. NC: Normal Control; ns: P>0.05; * p < .05; ** p < .01; *** p < .001.